Source Identification of Particulate Metals/Metalloids Deposited in the San Juan River Delta of Lake Powell, USA

Logan Frederick[1], William P. Johnson[1*], Thure Cerling[1], Diego Fernandez[1]

[1]Department of Geology and Geophysics, University of Utah, Salt Lake City, UT 84112, USA

Abstract

Whereas mining and non-mining sourced particulate metal/metalloids (PM) (<0.45 μm) are present in the tributaries of the San Juan River, USA, the individual contributions of PM from the San Juan River tributaries to the sediment of the San Juan River Delta of Lake Powell, USA were previously unknown. To determine these contributions, signatures of tributary PM, including enrichment factors, lead (Pb) isotopes, color, and particle size were used to tie layers in a San Juan River sediment core to upstream tributary sources. Tributary PM concentrations were determined for existing and newly-collected water quality samples by coupling these discrete measured elemental concentrations with total suspended solids concentrations. Discrete PM concentrations were categorized by runoff category (i.e., snowmelt, rainfall, and/or baseflow).

Average tributary PM concentrations that were uniquely elevated in a given tributary or during a given runoff category were used to establish enrichment factors, ratios of PM concentrations to aluminum (Al). Elevated ratios of Pb:Al, Cd:Al, Cu:Al, and Zn:Al in deposited sediment were linked to the Animas River. Elevated ratios of Ni:Al in deposited sediment were linked to the Mancos River and elevated ratios of Mn:Al in deposited sediment were linked to Chaco Creek. Pb isotope ratios in the sediment core spanned Pb isotope ratios measured in tributary suspended sediment; wherein the Pb isotope ratios reflected the depleted signature of the mineralized vein, the enriched signature of the Chinle Sandstone, or a mixture of these two endmembers. Sediment trap PM concentrations deployed over distinct runoff categories (i.e., baseflow with intermittent rainfall and peak snowmelt), were analyzed via principal component analysis (PCA) in order to link deposited sediment layers to runoff

Commented [LF1]: Pending

*Corresponding author: william.johnson@utah.edu

category by determining whether sediment trap layer PCA values fell within the 95% confidence interval probability ellipse of a tributary PM runoff category.

These independent lines of evidence were used to link probable tributary source and runoff category to sediment layers. The overall analysis indicated a single snowmelt layer was recorded in the sediment core, and that the 3.37 m San Juan River Delta core was deposited over ~1.3 years. Additionally, approximately 10% of the overall PM deposited in the sediment core was attributed to mining sources; whereas approximately 80% of the overall PM reflected a mixture of mining and non-mining sources.

Keywords: particulate metals/metalloid concentration, sediment cores, sediment traps, lead isotopes, principal component analysis

1. Introduction

1.1. San Juan River Delta Sediment

Following the 2015 Gold King Mine (GKM) spill, the US Environmental Protection Agency (USEPA) began remediating mining-sourced particulate metals/metalloids (PM) in the Bonita Peak Mining District, CO under Superfund (US Comprehensive Environmental Response, Compensation, and Liability Act) to improve water quality in the Animas River, CO (Figure 1) (USEPA, 2018). The Animas River is one of seven main tributaries to the San Juan River, each of which contributes mining and/or non-mining sourced PM (Abell, 1994; Church et al., 1997; Schemel et al., 2000; Clow, 2005; Larrick, 2010; Larrick and Ashmore, 2012; Dyer et al., 2016; Rodriguez-Freiere et al., 2016; Frederick et al., 2018). Whereas San Juan River PM are primarily deposited in the San Juan River Delta of Lake Powell, UT (Figure 1) (Hornewer, 2014), the overall contribution of mining and non-mining sourced PM from the tributaries of the San Juan River has previously been uncharacterized.

Sediment cores, which record PM deposition, also potentially record mining versus non-mining sourced PM in the San Juan River Delta. San Juan River Delta sediment layering suggests that changes in sediment source occurred over time, with visually distinct layers being associated with distinct elemental concentrations (Hornewer et al., 2014). Whereas resuspension events or diagenetic processes (e.g., redox) can alter sediment elemental concentrations following deposition (Ferrari, 1988; Pratson et al., 2008; Hornewer, 2014; Vernieu, 1997), the San Juan River tributaries mobilize distinct PM loads between tributaries and different runoff categories (i.e., snowmelt, rainfall, or baseflow) (Frederick et al., 2018). Because sedimentation rates in the San Juan River Delta are high and fluctuate annually as well as interannually (Standford and Ward, 1990; Potter and Drake, 1989; Vernieu, 2012), traditional sediment dating methods (e.g., cesium-137 or lead-210) are not reliable. In the absence of these dating procedures, we herein use geochemical signatures representing seasonal categories of runoff, where the record is punctuated by annual events such as snowmelt, as an alternative dating method. The overall objective of this paper is to use multiple lines of evidence developed from tributary PM geochemical signatures to differentiate mining versus non-mining sourced elemental concentrations in sediments of the San Juan River Delta. Additionally, tributary PM signatures indicative of snowmelt will be used to determine the age of a sediment core.

1.2. Source identification of elements deposited in lake sediment

In order to differentiate natural, industrial, and/or mining-sourced PM, sediment source identification in lacustrine systems has been performed using elemental concentrations in principal component analysis (PCA) (Christensen and Juarcek, 2001; Wang et al., 2015; Palau et al., 2012), lead (Pb) isotopes (Graney et al., 1995), and enrichment factors relative to conservative elements (Wang et al., 2015, Riba et al., 2002). Enrichment factors normalize concentrations of metals to conservative elements; e.g., iron (Fe), aluminum (Al), and can be used to determine inputs of anthropogenic and mining-sourced PM among contaminated and background lakes (Wang et al., 2015; Riba et al., 2002).

PCA is a statistical tool to reduce multidimensional datasets through the generation of principal components (PCs), which represent linear combinations of input variables (e.g., concentrations) (Li and Zhang, 2010; Wang et al., 2015). PCA performed with elemental concentrations was used to differentiate sources (e.g., mining, industrial, or natural), where sample categories occupied distinct PC space (Wang et al., 2015; Frederick et al., 2018). Additionally, PCA probability ellipses (also referred to as convex hulls), represent the confidence interval within PC space of a given sample category and can be used to predict categorical association of an independent data set (Palau et al., 2012). Stable isotopes of Pb, which do not fractionate during transport/deposition, have been utilized in both alluvial and lacustrine sediment to attribute sources (e.g., a mineralized vein) (Church et al, 1997, Frederick et al., 2018, Graney et al., 1995).

Overarching Hypothesis: Layers in sediment deposited in the San Juan River Delta of Lake Powell reflect distinct sources from upstream tributaries.

Hypothesis 1: Because elevations and lithologies range among tributaries, PM loads and PM concentrations from a given tributary change with runoff category (i.e. snowmelt, rainfall, or baseflow), yielding distinct layers in sediment traps and sediment cores at the downstream end of the system.

Hypothesis 2: Because mining tends to occur in high elevations, snowmelt-activated PM loads and PM concentrations tend to have elemental signatures; e.g., elevated Pb, cadmium (Cd), arsenic (As), zinc (Zn) and Pb isotope ratio (corresponding to mineralized vein) that can be used to link downstream sediment layers to mining origin. Underlying this approach is an assumption that negligible oxidative or reductive elemental mobilization occurred following deposition

2. Background

2.1. Tributaries of the San Juan River

The seven main tributaries of the San Juan River (Upper San Juan River, Animas River, La Plata River, Mancos River, McElmo Creek, Chaco Creek, and Chinle Creek) can be characterized by prevalence of

precious metal mining, predominant underlying geologic unit, as well as runoff type (i.e., snowmelt, rainfall, or baseflow) in the tributary (Supporting Information Figure SI1). Mined tributaries, defined as >50 precious metal mines, include the Animas, Upper San Juan, Mancos, and La Plata Rivers; whereas unmined tributaries, defined as <50 precious metal mines, include McElmo, Chinle, and Chaco Creeks. The watersheds of McElmo Creek, Mancos River, and La Plata River are predominantly underlain (>50% area) by the Mancos Shale, a Cretaceous-age marine shale naturally high in As and Se (Dryer et al., 2016; US Department of Energy, 2011; Larrick and Ashmore, 2012); whereas the watersheds of Chinle Creek and Chaco Creek are predominantly underlain (>50% area) by the Chinle Sandstone, a Pennsylvanian to Cretaceous age sandstone naturally high in Al, As, cobalt (Co), chromium (Cr), Fe, vanadium (V), and Zn (Newman, 1962) (Supporting Information Figure SI1). Stream hydrographs in snowmelt-dominated watersheds (Upper San Juan and Animas) are characterized by sustained high flow during spring, whereas hydrographs from rainfall-dominated watersheds (La Plata, McElmo, Chinle, and Chaco) are characterized by short high intensity flow events. Additional information characterizing prevalence of mining, underlying geologic units, and runoff in the San Juan Watershed is available in Frederick et al. (2018).

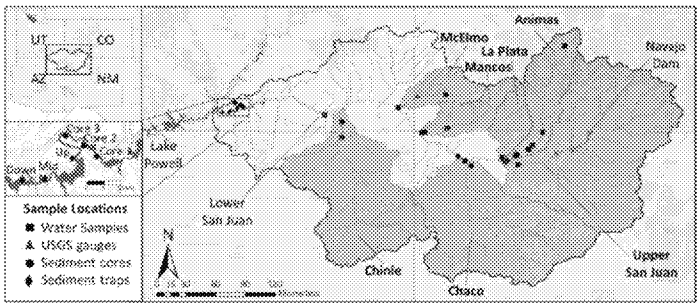

Figure 1. Map of the San Juan Watershed located in Four Corners, USA. Tributary watersheds are outlined and labeled in black. Locations for surface water samples (black squares), USGS stream gauges (red triangles), USGS sediment cores (black circles), and USGS sediment traps (black diamonds) are shown. USGS sediment cores were

collected at USGS sites 0364200, 0382600, and 0410700, for cores 1, 2, and 3, respectively. USGS sediment traps were collected downstream of Mexican Hat, UT at upstream, mid-stream, and downstream locations. A map with watershed mining activity and geology is given in the Supporting Information (Figure SI1).

A previous study on source identification of PM loads (mg_{metal}/sec) in the tributaries of the San Juan River (Frederick et al., 2018) found that PM loads vary with runoff category (i.e. snowmelt, rainfall, or baseflow), indicating that different runoff categories represent different PM sources within a watershed. PM loads mobilized during snowmelt reflected high elevation terrain, whereas PM loads mobilized during rainfall reflected PM sourced from all elevations (Frederick et al., 2018). The Animas River (Figure 1), dominated PM load contributions to the San Juan River during snowmelt; where large PM loads of Pb, As, copper (Cu), and Zn were attributed to mining in the Animas headwaters (Frederick et al., 2018). Chinle and Chaco Creek, two tributaries with no precious metal mining (Figure 1), dominated PM load contributions to the Lower San Juan River during rainfall; where large PM loads of Al, Co, Cr, Fe, V, and Zn were attributed to the Chinle Sandstone (Frederick et al., 2018).

PM Pb isotope ratios from mined San Juan River tributaries generally reflected Pb isotopes in the mined mineralized vein (Church et al., 1997); whereas Pb isotope ratios in unmined tributaries reflected the predominant underlying geologic unit (Frederick et al., 2018). The Animas, Upper San Juan, La Plata and McElmo Rivers had Pb isotope ratios (Frederick et al., 2018) that reflected the mineralized vein (Church et al., 1997), which is present in the headwaters of each tributary except McElmo Creek. The Dolores River, headwaters underlain by the mineralized vein, is diverted to McElmo Creek to maintain year-round flow (Larrick, 2010) and appears to dominate the McElmo Pb signature. The Mancos River Pb isotope ratios reflected a combination of the mineralized vein and the Mancos Shale, which has relatively enriched $^{208}Pb/^{204}Pb$ and $^{206}Pb/^{204}Pb$ (Church et al., 1997). Chinle and Chaco Creeks Pb isotope ratios reflected the enriched $^{208}Pb/^{204}Pb$ and $^{206}Pb/^{204}Pb$ Chinle Sandstone (Frederick et al., 2018).

Commented [WPJ2]: Pending.

146 *2.2. San Juan River Delta of Lake Powell*

147 Lake Powell, the second largest reservoir in the USA (US Bureau of Reclamation, 2012), impounds
148 the Colorado, Escalante, and San Juan Rivers at the border of Utah and Arizona (Figure 1). These three
149 rivers annually supply an average of 60 million metric tons of sediment to Lake Powell (Potter and
150 Drake, 1989), with a majority of the sediment and water (~96%) sourced from the Colorado and San
151 Juan Rivers (Irons et al., 1965; Evans and Paulson, 1983). Sediment deposition of alluvial loads occurs
152 mainly at the reservoir inflows; where coarse material is deposited in the upstream portion of the delta
153 and finer material is deposited downstream as a function of decreasing water velocity (Vernieu, 1997).
154 Finer material is characterized by large surface areas with active sites for ion exchange or sorption of
155 elements (Vernieu, 1997). Mobilization of elements in Lake Powell sediment may also occur during
156 prolonged drought; e.g. from 1988 to 1993, where over 100 km of deltaic sediment was exposed
157 (Vernieu, 1997).

158 In order to document the presence of elevated elemental concentrations in San Juan River deltaic
159 sediment, the United States Geological Survey (USGS) collected three sediment cores in August 2010
160 ranging in depth from 1.48 to 4.6 m (Hornewer, 2014) (Figure 1). The three sediment cores (USGS
161 371712110364200, USGS 371425110382699, and USGS 371545110410700) showed variation in
162 elemental concentration with depth; however, a sediment accumulation history was not determined
163 (Hornewer, 2014).

164 Additionally, in 2015 the USGS deployed sediment traps at three locations (upstream, mid-stream,
165 and downstream, Figure 1) in the San Juan River Delta during baseflow with intermittent rainfall and
166 snowmelt (Figure 2) (UDWQ et al., 2018). Lower San Juan River baseflow conditions punctuated by four
167 rainfall events in the watershed were captured in 48 cm at the upstream location from 8/23/2015 to
168 11/19/2015 (USGS MRP-15078). Snowmelt runoff in the Lower San Juan River (5/17/2016 to 7/14/2016)
169 was captured with three sediment traps (upstream, mid-stream, and downstream locations), where 12.7

cm were deposited in each trap over 59 days (USGS MRP-15597). Lower San Juan River baseflow conditions punctuated by a large rainfall event and two smaller rainfall events in the watershed (7/14/2016 to 10/26/2016) were captured in 3.5, 6, and 2 cm from the upstream, mid-stream, and downstream locations, respectively (USGS MRP-16105).

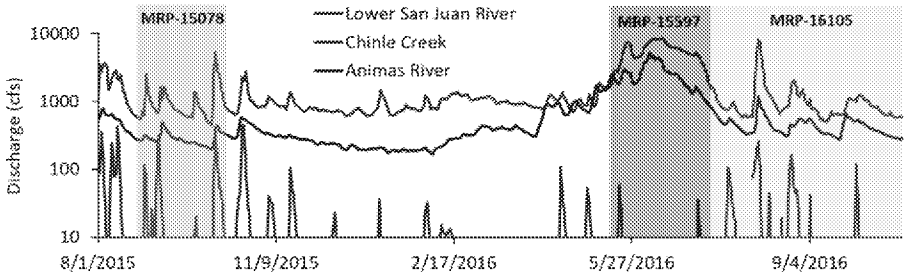

Figure 2. Periods over which the USGS deployed sediment traps in the Lower San Juan River: baseflow with intermittent rainfall 2015 (MRP-15078), snowmelt 2016 (MRP-15597), and baseflow with intermittent rainfall 2016 (MRP-16105). Hydrographs for the Lower San Juan River (solid line, 09379500), Animas River (blue line, 0964500), and Chinle Creek (red line, 09379200) (USGS, 2018) are shown.

Sediment deposition rates in Lake Powell are high (m per year range) and vary substantially within and between years (Standford and Ward, 1990; Potter and Drake, 1989; Vernieu, 2012). For example, USGS sediment traps collected during baseflow with intermittent rainfall show interannual variation in deposition rates, e.g., 1.97 m/year in 2015 and 0.21 m/year in 2016. Average sediment accumulation rates in the San Juan River Delta were reported to range from 0.48 m/year to 2 m/year (Potter and Drake, 1989; Standford and Ward, 1990; Vernieu, 2012). The high observed sedimentation rates in the San Juan River Delta lead to an expectation that the USGS sediment cores (ranging in length from 1.48 m to 4.6 m) likely represent less than a decade of sediment deposition. Whereas cesium (Cs)-137 and Pb-210 isotopes are commonly used to determine sediment accumulation rates in modern lake records

(post-1950) (e.g., Mahler et al., 2005; Bloesch and Evans, 1982; USGS, 2016); the combination of fluctuating deposition rates and the decade (short) timescale make traditional dating methods unfeasible. Therefore, seasonal signatures of San Juan River tributaries may help in estimation of deposition time in the San Juan River Delta sediment cores.

3. Methods

The concentration of total and filtered metals (<0.45 μm), and total suspended solids (TSS) for each of the seven tributary watersheds and the main channel of the San Juan River were obtained from the USEPA Storage and Retrieval database (STORET) (USEPA, 2017) (Figure 1) and supplemented with opportunistic samples as described in Frederick et al. (2018). Water quality samples in STORET were collected as grab samples in the shallow water column, which can neglect PM in the deeper water column. However, direct comparisons between shallow grab samples and samples composited across water column depth collected May to July 2016 and 2017 from the Lower San Juan River, found <10% difference in metal concentrations between these two sampling methods, demonstrating that grab samples adequately capture mobilized PM under the conditions in which this comparison was made (UDWQ et al., 2018).

Supplemental water quality samples were analyzed for total and filtered elemental concentrations and Pb isotopes using an Agilent 7500ce quadrupole ICP-MS with collision cell and Neptune Plus multicollector, respectively as described in Frederick et al. (2018). Both PM loads (mg_{metal}/sec) and PM concentrations (mg_{metal}/mg_{sed}) were determined for the analyzed samples; where PM loads were examined in Frederick et al. (2018) and PM concentrations are examined here.

PM concentrations (mg_{metal}/mg_{sed}) were determined for each sample by differencing total and filtered concentrations divided by the TSS concentration. Samples were categorized and averaged according to runoff category (i.e., snowmelt, rainfall, or baseflow) as described in Frederick et al. (2018), under the assumption that each sample mobilized PM concentrations representative of the assigned

runoff category. Student's t-tests (unpaired, two-tailed, unequal variance) were used to determine whether average PM concentrations were distinct ($p < 0.05$) between tributary or among runoff categories within a given tributary.

The three sediment cores collected from the San Juan River Delta of Lake Powell in August 2010 (Core 1, Core 2, and Core 3) (Figure 1) (Hornewer, 2014) had individual thickness of 1.48 m, 3.37 m, and 4.60 m, respectively. The complete sampling methodology and coring procedure are given in Hornewer (2014) and Hart et al. (2005). Various strata were subsampled (20, 32, and 49 subsamples, for cores 1, 2, and 3, respectively), dried, digested via total digestion (HCl, HNO_3, $HClO_4$, and HF at low temperature) and analyzed via Inductively Coupled Plasma Atomic Emission Spectrometry (ICP-AES) (Hornewer, 2014).

Additional sediment samples were sub-sectioned from the frozen cores in Fall 2017 at the USGS laboratory in Boulder, CO (6, 19, and 15 samples from cores 1, 2, and 3, respectively). Because the three sediment cores have similar average elemental concentrations (student t-test $p > 0.05$) (Supporting Information, Figure SI2), Core 2 was selected and analyzed for elemental concentration and Pb isotopes via ICP-MS with a 10% HCl digestion. Grain size was analyzed via Sympa Tec Lixell Helos/KF laser diffraction using two lenses, which captured particles sizes 0.25 µm to 87.5 µm and 0.5 µm to 350 µm, respectively. Particle sphericity was analyzed via Sympa Tec Lixell QICPIC. Sediment color was assigned based on Munsell Soil Color Charts (Munsell Color x-rite, 2009). Water content and bulk density of the sediment samples were determined by weighing a known volume of sample before and after drying. Elemental concentrations were then corrected to represent the dry elemental concentration. A 10% HCl digestion was assumed to extract only the metal/metalloid coating on the mineral (extractable phase), rather than the entire mineral matrix (total digestion). In this way, PM concentrations in the water, also digested via 10% HCl, can be directly compared to sediment elemental concentrations.

Sediment traps were sub-sectioned and analyzed by the USGS (UDWQ et al., 2018); where layers deposited during rainfall/baseflow 2015 were sub-sectioned into 10 samples at 4 to 5 cm increments.

Sediment deposited during peak snowmelt at the upstream location was sub-sectioned by visual layer (total of 3 subsections), whereas the sediment from the other two locations was homogenized. Sediment deposited during rainfall/baseflow 2016 was homogenized and analyzed separately for each trap location. All sediment trap samples were dried, digested via total digestion and analyzed via ICP-AES-MS multi-acid (ICP-42) (USGS method 19-42, USGS, 2018).

PCA was performed in R (R Core Team, 2013) to generate linear combinations of sediment elemental concentrations; where PC1 accounts for the majority of variance among elemental concentrations, and PC2 accounts for the largest remaining variance orthogonal to PC1. Because sediment elemental concentrations spanned multiple orders of magnitude, elemental concentrations were log transformed to avoid overweighting of large concentrations. PCA was performed for the sediment trap elemental concentrations in order to generate runoff-specific probability ellipses representing 95% confidence interval. PC1 and PC2 weights were then applied to log-transformed sediment core elemental concentrations (also measured via total digestion).

Through utilizing enrichment factors, PCA, and Pb isotopes as independent lines of evidence, the source identification of San Juan River Delta sediment layers can be determined. Enrichment factors, Pb isotopes, sediment color, and grain size tie sediment deposited in the San Juan River Delta to upstream tributaries; where enrichment factors, Pb isotopes, and color will characterize the bioavailable/redox sensitive component of sediment (extractable phase). Enrichment factors and color of San Juan River Delta sediment layers may record changes in PM source, where distinct PM concentrations and/or color exists between tributaries or between runoff categories (assuming no diagenetic processes). Pb isotopes in San Juan River Delta sediment may reflect the mineralized vein (sourced from mined tributaries), predominant underlying geologic unit (sourced from unmined tributaries), or a combination of sources. Sediment trap elemental concentration PCA (total digestion) establishes runoff category trends in deposited sediment to be used predictively for San Juan River Delta sediment.

263

264 **4. Results/Discussion**

265 *4.1. Signatures in extractable phases*

266 Tributary PM concentrations that were uniquely elevated in a given tributary or during a given
267 runoff category within a given tributary were used to establish enrichment factors for comparison to
268 those from San Juan River Delta sediment. For each runoff category, distinctly elevated PM
269 concentrations were correlated with specific tributaries. Cd, Cu, Pb, selenium (Se), and Zn PM
270 concentrations were higher in the Animas River relative to other tributaries during all runoff categories
271 ($p<0.05$, Figure 3; Supporting Information Figure SI3). Animas River rainfall/baseflow beryllium (Be) and
272 molybdenum (Mo) PM concentrations were greater than other tributary rainfall or baseflow PM
273 concentrations (Figure 3 upper and lower panel). Additionally, Animas River snowmelt As, manganese
274 (Mn), and Mo PM concentrations were greater than other tributary snowmelt PM concentrations
275 (Figure 3 middle panel). Mancos River snowmelt Be, Cr, and nickel (Ni) PM concentrations and baseflow
276 Mo PM concentrations exceeded other tributary PM concentrations for the respective runoff categories
277 (Figure 3 middle and lower panel). During rainfall, Chaco Creek Mn concentrations were greater than
278 other tributary watersheds (Figure 3 upper panel).

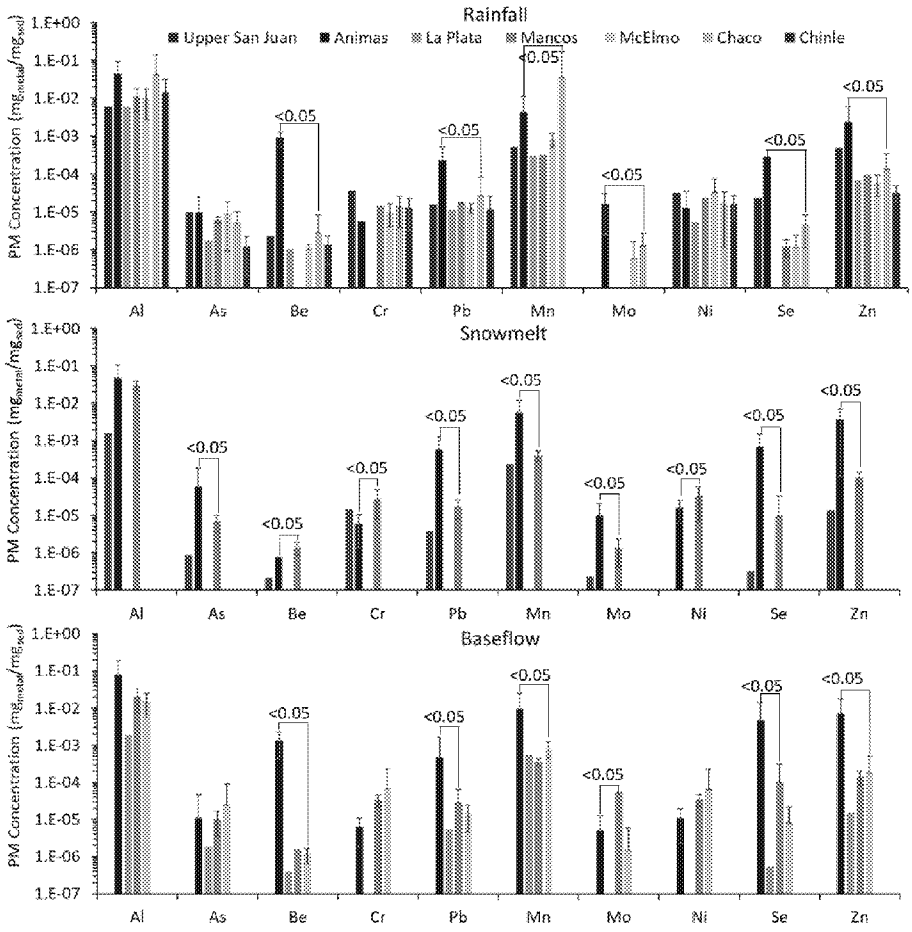

279

280 **Figure 3**. Average PM concentration in the tributary watersheds during rainfall (upper panel), snowmelt

281 (middle panel), and baseflow (lower panel) shaded from upstream (dark blue) to downstream (red).

282 Statistically significant differences ($p<0.05$) between average PM concentrations are shown. Tributary

283 PM concentrations are only present for runoff categories occurring within the tributary (e.g., no Chinle

284 baseflow PM concentrations exist). PM concentrations not shown in Figure 4 are given in Supporting

285 Information (Figure SI3).

Whereas PM concentrations were generally indistinct between runoff categories within a given tributary (Figure 4; Supporting Information Figure SI4), a few exceptions existed which differentiated tributary snowmelt PM concentrations from rainfall or baseflow PM concentrations. These exceptions included: Animas River As PM concentrations, which were greater for snowmelt relative to rainfall and baseflow ($p < 0.05$) (Figure 4) as well as Animas River Se PM concentrations, which were greater for baseflow relative to snowmelt and rainfall ($p < 0.05$) (Figure 4). Additionally, Mancos River Mo and Se PM concentrations were greater for snowmelt relative to rainfall or baseflow (Supporting Information, Figure SI4), although elevated Mancos River snowmelt Mo and Se PM concentrations were insignificant compared to Animas River Mo and Se PM concentrations (Figure 3).

Because the timing of Lake Powell sediment deposition was unknown, PM concentrations that were uniquely elevated in a given tributary or during a given runoff category in a given tributary can be used to determine the source or timing of deposition. Elevated PM concentrations of Cd, Cu, Pb, and Zn were indicative of Animas River contributions, whereas elevated As and Se concentrations were indicative of Animas River snowmelt contributions. Elevated Ni PM concentrations were indicative of Mancos River snowmelt contributions, and elevated Mn PM concentrations were indicative of Chaco Creek rainfall contributions. That PM Al concentrations were similar between tributaries (Figure 3) and between runoff category (Figure 4), justifies the use of Al as a conservative element for enrichment factors in the San Juan River.

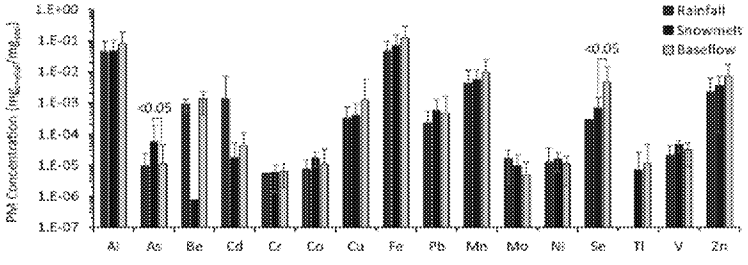

Figure 4. Average PM concentrations (mg_{metal}/mg_{sed}) in the Animas River during rainfall (red), snowmelt (blue), and baseflow (grey). Statistically significant differences ($p < 0.05$) between average PM concentrations are shown.

For elements with unique tributary or runoff PM concentrations (e.g., As, Se, and Pb), enrichment factors were calculated relative to Al for sediment Core 2; where variations in these ratios with depth were examined to indicate potential changes in PM sources (Figure 5B). Sample 2-03 had the greatest Pb:Al, Cu:Al, Cd:Al, and Zn:Al ratios, suggesting Animas River-sourced PM (Figure 5B; Supporting Information, Figure SI5). Peaks in Ni:Al occurred in samples 2-11 and 2-14, suggesting Mancos River-sourced PM (Figure 5B). Sample 2-05 also had a peak in Ni:Al co-occurring with a peak in Cd:Al, Cu:Al and As:Al indicating a mixture of sources (Figure 5B). Peaks in Mn:Al occurred in samples 2-03, 2-06 and 2-12, suggesting Chaco Creek sourced PM (Supporting Information, Figure SI5).

Core 2 sediment color and grain size corresponded to ranges observed in PM in upstream tributaries. Core 2 sediment was predominantly brown (Munsell color 4/3), red (Munsell color 4/6), and dark brown (Munsell color 3/4) (Munsell Color x-rite, 2009) (Figure 5A). Similar colors were observed in PM from the tributaries; where suspended sediment in the Animas River, Upper San Juan River, Mancos River, La Plata River, and McElmo Creek ranged from brown (Munsell color 4/3) to dark brown (Munsell color 3/4) and suspended sediment in Chinle Creek was red (4/8) (Munsell Color x-rite, 2009) (Supporting Information, Figure SI6). The exception was Chaco Creek, which was light olive brown (Munsell color 5/4), a color not observed in Core 2. Under the assumption that diagenetic processes did not alter sediment color following deposition, the red color in samples 2-01, 2-12, 2-13, 2-15, and 2-18 (Figure 5A) may reflect sediment sourced from Chinle Creek.

Median (P50) grain size in Core 2 ranged from 4 μm to 150 μm with a majority of the sediment <10 μm in size (Figure 5C). Median grain size was used because particles were observed over the entire size range (0.25 μm to 87.5 μm or 0.5 μm to 350 μm, dependent on lens used) and were not normally

distributed (Supporting Information, Figure SI7). The median suspended sediment size in Chinle and Chaco Creeks were smaller than those observed in sediment Core 2 (P50 2.9± 0.12and 3.4± 0.05 µm, respectively), while Upper San Juan River, Animas River, Mancos River, La Plata River, and McElmo Creek mobilized particles with median size ranging from 8.5 µm to 39.0 µm (Frederick et al., 2018). Core 2 sphericity measurements were not useful in differentiating tributary source (mean sphericity 0.71 ±0.01) and are provided in the Supporting Information (Figure SI8)

Sediment elemental concentrations in the extractable phase were 1 to 1000 times lower than those determined by dissolution of the matrix (Hornewer, 2014) (Figure 5D). In general, over 50% of elemental concentration was in the sediment matrix and not on the coating, with less than 10% of Al, Cr, Sb, and V on the coating (Figure 5D).

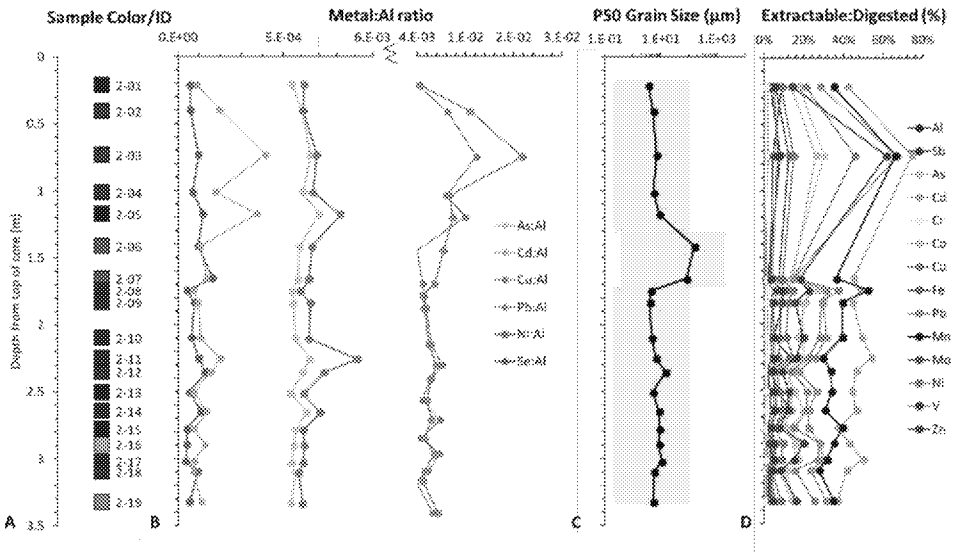

Figure 5. A) Dominant Munsell color of sediment (Munsell Color x-rite, 2009) and sample ID as a function of depth from the top of the core (m); B) ratio of extractable As (gold), Cd (orange), Cu (green), Pb (light blue), Mo (dark blue), Ni (purple), and Se (pink) to Al as a function of depth from the top of the

core (m); C) Median (P50) grain size (μm) for samples (black line) as a function of depth from the top of the core (m) with the lens size range in grey; and D) Percent of metal in extractable phases relative to full digestion as a function of depth from the top of the core (m). The lesser number of samples in D reflects lesser samples fully digested (Hornewer, 2014).

Similar to elemental concentrations, color, and grain size, sediment Pb isotope ratios linked deposited sediment to PM in upstream tributaries. Pb isotope ratios in Core 2 spanned Pb isotope ratios measured in tributary suspended sediment (Frederick et al., 2018); where Pb isotope ratios for samples 2-02 and 2-03 reflected the mineralized vein, and samples 2-01, 2-12, 2-13, 2-15, and 2-18 reflected the Chinle Sandstone (Figure 6). Pb isotopes measured in 2-04 and 2-05 represented a transition, similar to the Pb isotope ratios measured in the Mancos River (Figure 6).

Commented [LF3]: Pending

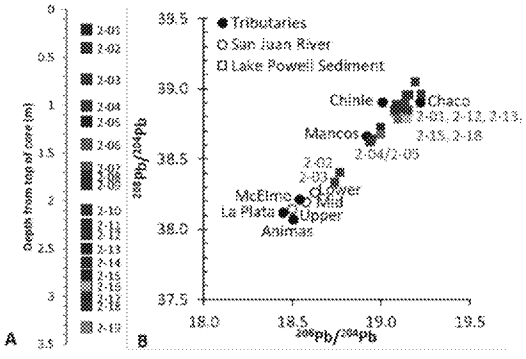

Figure 6. A) Dominant Munsell color of sediment (Munsell Color x-rite, 2009) and sample ID as a function of depth from the top of the core (m); B) Pb isotope ratios for the tributaries (closed circles), San Juan River (open circles), and Lake Powell Sediment (squares). Sediment are colored based on dominant Munsell color of sediment.

4.2. Sediment matrix signatures in PCA space

Runoff category signatures were established through PCA of sediment trap PM concentrations (via total digestion) (mg_{metal}/mg_{sed}), which were deployed during baseflow with intermittent rainfall and peak snowmelt (UDWQ et al., 2018). Sediment trap periods occupied distinct PC spaces (Figure 7A); where sediment deposited during snowmelt had higher Pb, Zn, V, Mo, and As concentrations (lower PC1) than sediment deposited during baseflow with intermittent rainfall, which were higher in Fe, Al, and Ni concentrations (higher PC1) (Figure 7A). Rainfall/baseflow sediment deposited in 2015 had higher Fe, Al, and Ni concentrations (higher PC1) than sediment deposited during rainfall/baseflow in 2016 (Figure 7A), possibly reflecting the larger 2015 rainfall events resulting in significant flow in Chinle Creek (Figure 2) (UDWQ et al., 2018). Additionally, the significantly higher sedimentation rate captured in 2015 rainfall/baseflow trap than 2016 rainfall/baseflow trap (1.97 m/year versus 0.21 m/year, respectively), indicates the activation of a large sediment source (e.g., Chinle Creek) during the 2015 deployment.

Sediment trap periods were not further differentiated in PC2, as sediment deposited during both snowmelt and baseflow with intermittent rainfall spanned PC2 (Figure 7A). Unlike sediment trap period, sediment trap location (upstream, midstream, and downstream) did not occupy distinct PCA spaces (Figure 7A), where colors corresponding to sediment trap location were mixed throughout the PCA space.

Core 2 sediment PM concentrations (total digestion), occupied similar PCA space to sediment traps; excepting 2-07 which was lower in all PM concentrations (Figure 7B). Samples 2-01, 2-13, 2-15, 2-17, and 2-18 occupied PC space within the probability ellipse assigned to 2015 rainfall/baseflow sediment traps, indicating that these sample concentrations were similar (95% confidence) (Figure 7B). Whereas samples 2-03 and 2-16 occur outside the probability ellipse for peak snowmelt sediment, these samples occupied a similar PC2 space (higher Pb, Zn, Mo, and As) as that occupied by early and peak snowmelt samples (Figure 7B). Samples 2-09 and 2-19 occurred in the 2016 rainfall/baseflow probability ellipse, indicating similar concentrations (Figure 7B).

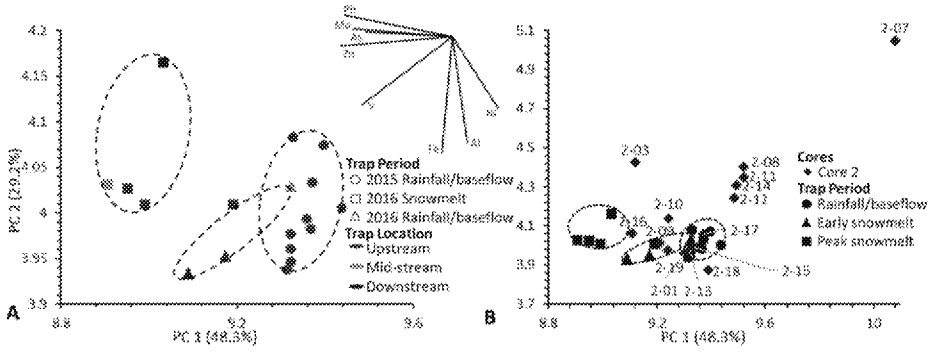

Figure 7. A) PCA for USGS sediment traps deployed over three periods: 2015 rainfall/baseflow (circles), 2016 snowmelt (squares), and 2016 rainfall/baseflow (triangles), collected at three locations: upstream (red), mid-stream (green), and downstream (blue) (Figure 1). Graphical representation of elemental PC weights (solid lines) are given, where vectors denote weight and direction of PC1 and PC2 weights. PC1 and PC2 explained 48.3% and 29.2% of the variance, respectively. PC3 explained 14.5% of the variance and is shown in the supporting information, Figure SI9; B) Sediment core samples were assigned PC1 and PC2 weights generated by sediment traps (blue diamonds) and graphed with sediment deposited during 2015 rainfall/baseflow (black circles), 2016 snowmelt (squares), and 2016 rainfall/baseflow (triangles). Probability ellipses, representing the 95% confidence interval, are given for the distinct sediment trap categories.

4.3. Linking Sediment Core Layers to PM of Upstream Tributaries

Elemental and isotopic signatures in Lake Powell sediment were linked to those of PM in upstream tributaries. The 0.66 m layer near the top of Core 2, represented by samples 2-02 and 2-03, likely reflected Animas River snowmelt PM; where the Pb isotope ratios represented the mineralized vein present in the headwaters of the Animas River (Figure 6), ratios of Pb:Al, Cd:Al, Cu:Al, and Zn:Al were characteristic of the Animas River (Figure 5B), and elemental concentrations occupied similar PC space

404 as sediment deposited during snowmelt (Figure 7). The dominance of the Animas River PM signature to
405 the Lower San Juan River during snowmelt (Frederick et al., 2018) in addition to the low deposition rates
406 modelled in the San Juan River during high flow typical of snowmelt (Sullivan et al., 2017), would allow
407 Animas River snowmelt PM signatures to be deposited as a layer in the sediment of the San Juan River
408 Delta. The 0.24 m layer deposited before the snowmelt layer, represented by samples 2-04 and 2-05,
409 possibly reflected Animas River early snowmelt PM as the Pb isotope ratio was mixed (Figure 6), but no
410 excursions in elemental concentration were noted.
411 Sediment core layers with enriched Pb isotope ratios (Figure 6), red color (Figure 5), and enriched
412 Mn:Al (Supporting Information Figure SI5) likely reflected Chinle and Chaco Creek PM sources (i.e.,
413 layers represented by samples 2-01, 2-12, 2-13, 2-15, 2-17, and 2-18). These samples also had elemental
414 concentrations that occupied similar PC space as sediment deposited during 2015 rainfall/baseflow
415 (Figure 7), suggesting the dominance of Chinle Creek PM during large rainfall events. That Chinle Creek
416 (farthest downstream tributary at ~20 km upstream of Lower San Juan) dominated rainfall layers
417 deposited in the San Juan River Delta sediment, indicates that short duration high intensity flow events
418 transmit PM across (~20 km) the system. Whereas the red color of Core 2 layers could potentially reflect
419 post-depositional oxidation of iron, it more likely reflects the red color of Chinle Creek PM, since PCA
420 and Pb isotope ratios for red sediment layers also suggested Chinle Creek as a source.
421 The 0.57 m thick sandy layer, represented by samples 2-06 and 2-07, cannot be attributed to a
422 runoff category because PM concentrations were lower than those measured in any sediment trap
423 (Figure 7); however, the Pb isotope ratios were representative of the Chinle Sandstone (Figure 6). The
424 median grain size of the sandy layer (154 μm and 90 μm, for sample 2-06 and 2-07 respectively) (Figure
425 5C) was larger than any median tributary particle size, suggesting that events mobilizing coarse sand
426 particles were rare, or that coarse particles were not successfully collected using the grab sampling
427 technique in upstream tributaries. Either possibility is consistent with the good agreement in PM

concentrations measured between sampling composited and grab samples (UDEQ et al., 2018), since coarse particles have low extractable elemental concentrations (Figure 5D). Notably, no sand layers were observed in sediment traps, suggesting that coarse particles were not suspended in the water column.

Other layers likely reflect a mixture of sources deposited during baseflow; where sediment PM concentrations were lower than both baseflow with intermittent rainfall and snowmelt (Figure 7) and Pb isotopes were enriched compared to the Chinle Sandstone (Figure 6) (i.e., samples 2-08, 2-11, 2-14, and 2-19). Sediment core sample 2-16 occupied similar PC space as sediment deposited during snowmelt but had a Pb isotope ratio reflective of the Chinle Sandstone, potentially indicating a mixture of sources.

Because Animas River snowmelt PM loads in the San Juan River have been attributed to mining in the headwaters of the Animas River (Frederick et al., 2018), sediment layers reflecting the Animas River snowmelt signature were also attributed to mining sources. Conversely, because rainfall PM loads sourced from the Chinle and Chaco tributaries have been attributed to non-mining sources (Frederick et al., 2018), sediment reflecting Chinle and Chaco Creek rainfall signatures were attributed to non-mining sources. Therefore the percent of PM sourced from mining and non-mining sources was estimated from the known percent contribution of mining and non-mining sourced PM in the Lower San Juan River (Frederick et al., 2018), the length of each sediment layer (Hornewer, 2014), and bulk density (Supporting Information, Figure SI10) of each sediment layer. Assuming each subsample PM concentration represented the average PM concentration for a given layer, the percent of mining and non-mining sourced PM over Core 2 was calculated. For Core 2, 0.2% Al, 4% As, 5% Cu, 1% Fe, 10% Pb, and 8% Zn was attributed to mining sources and 5% Al, 2% As, 7% Cu, 1% Fe, 3% Pb, and 4% Zn was attributed to non-mining sources.

4.4. Age of the Core

Our results suggest that Core 2 was deposited in only ~1.3 years, which reflects the high sedimentation rates reported to occur during some years in the San Juan River delta. Core 2 was collected in mid-August 2010, indicating that the 2010 snowmelt signature was represented in samples 2-03 to 2-04 (near the top of the record). No other snowmelt layer was detected in Core 2, suggesting that the 2009 snowmelt was not represented. 2009 was a low snowmelt year in the Lower San Juan River, with peak flow ending in early May rather than the typical June or July (Supporting Information Figure SI10), (USGS, 2018). Core 2 was collected directly after a large precipitation event (08/03/2010) where flow in the Lower San Juan River exceeded 5000 cfs (USGS, 2018), and flow in Chinle Creek reached ~100 cfs, likely yielding the layer represented by sample 2-01. A similar age for this core, 1.4 years, was determined using bathymetric survey elevation and average sedimentation rates (UDWQ et al., 2018).

Whereas Pb isotopes, particle sizes, and enrichment factors were determined for Core 2, these attributes were not determined for Cores 1 and 3. PCA was performed for Cores 1 and 3 (Supporting Information, Figure SI11). Both Core 1 and Core 3 had a single sample fall within the probability ellipse established by 2016 snowmelt, and multiple samples fall within the probability ellipses established by 2015 and 2016 rainfall/baseflow sediment traps. Future work will examine the record provided in these sediment cores.

The detection of an Animas River snowmelt layer in Core 2 suggests that high flow, typical of spring runoff, is needed for upstream signatures (above Chinle Creek) to be preserved in the downstream sediment record. Despite co-occurring high flow resulting from Navajo Dam release, the GKM event was not likely preserved as a layer in the San Juan River Delta, as GKM PM was mainly (~90%) deposited in Animas River (Sullivan et al., 2017).

5. Conclusions

San Juan River Delta sediment PM reflects mining and non-mining sources from the tributaries of the San Juan River. Tributary Pb isotopes and PM concentrations, which differ with runoff category, were used to link sediment core layers to upstream tributaries; where the 3.37 m core examined here represented approximately 1.3 years of sediment deposition. Approximately 10% of the overall PM deposited in the sediment core was attributed to mining sources, with ~80% of the overall PM reflecting a mixture of mining and non-mining sources.

References

Abell, Robin. San Juan River Basin Water Quality and Contaminants Review. 1994 volume 1. Museum of Southwester Biology.

Bloesch, J and Evans, R.D. (1982) Lead-210 dating of sediments compared with accumulation rates estimated by natural markers and measured with sediment traps. *Hydrobiologia* 92:579-586.

Christensen, V.G. and Juracek, K.E. Variability of metals in reservoir sediment from two adjacent basins in the central Great Plains. *Environmental Geology* 2001. 40 (4-5) 470- 481.

Church, S.E.; Kimball, B.A.; Fey, D.L.; Ferderer, D,A; Yager, T.J; Vaughn, R.B. Source, Transport, and Partitioning of Metals between Water, Colloids, and Bed Sediment of the Animas River, Colorado. 1997. United States Geological Survey 97-151.

Clow, Scott and Stephens, Daniel B. Nonpoint Source Assessment of the Ute Mountain Ute Reservation of Colorado, New Mexico and Utah. 2005. Ute Mountain Ute Tribe and Stephens and Associates, Inc.

Dyer, Melissa; Moore, Stephen A.; Stumpf, Stacy E. Water Quality Monitoring for the Mancos River in Mesa Verde National Park: 2012-2013 Summary Report. 2016. National Park Service: Natural Resource Data Series NSP/SCPN/NRDS-2016/1221.

Evans, T. D., and Larry J. Paulson. "The influence of Lake Powell on the suspended sediment-phosphorus dynamics of the Colorado River inflow to Lake Mead." (1983): 57.

Ferrari, R.L. 1988. 1986 Lake Powell Survey. U.S. Burau of Reclamation Rep. REC-ERC-88-6. NTIS, Springfield, VA.

Frederick, Logan; Cerling, Thure; Fernandez, Diego; VanDerslice, James; Johnson, William. 2018. Differentiating mining and non-mining sourced contaminants in the tributaries of the San Juan River, USA. In preparation.

Graney, J.R.; Halliday, A.N.; Keeler, G.J.; Nriagu, J.O.; Robbins, J.A.; Norton, S.A. (1995) Isotopic records of lead pollution in lake sediments from northeastern United States. *Geochmica et Cosmochimica Acta*. 50(9)1715-1728.

Hornewer, N.J. Sediment and Water Chemistry of the San Juan River and Escalate River Deltas of Lake Powell, Utah, 2010-2011. United States Geologic Survey. 2014-1096.

Hart, R.J, Taylor, H.E., Antweiler, R.C., Graham, D.D., Fisk, G.G., Riggins, S.G., and Flynn, M.E., 2005, Sediment chemistry of the Colorado River delta of Lake Powell, Utah, 2001: U.S. Geological Survey Open-File Report 2005-1178, 33 p.

Irons, W.V., Hembree, C.H., and Oakland, G.L. 1965. Water resources of the Upper Colorado River Basin. Technical report: Washington, D.C., U.S. Geological Survey Professional Paper 441, 370 p.

Larrick, Colin and Ashmore, Jamie. Mancos River Water Quality and Trends Assessment: 2011 – 2012. Ute Mountain Ute Tribe.

Larrick, Colin. McElmo Creek, Lower San Juan River, Colorado and Cottonwood Wash, Utah Water Quality and Trends Assessment: 2009 – 2010. 2010.

Li, Siyue and Zhang, Quanfa. Risk assessment and seasonal variations of dissolved trace elements and heavy metals in the Upper Han River, China. 2010. *Journal of Hazardous Materials*. 181, 1051-1058.

Malher, Barbara; Can Metre, Peter C.; Callender, Edward. 2006. Trends in metals in urban and reference lake sediments across the United States, 1970 to 2001. *Environmental Toxicology and Chemistry* 25(7)1698-1709.

Munsell Color x-rite. Munsell Soil Color Charts with Genuine Munsell Color Chips; 2009 [Year Revised, 2009, Munsell Color 4300 44th Street, Grand Rapids, MI 49512, USA].

Newman, William L. Distribution of Elements in Sedimentary Rocks of the Colorado Plateau- A Preliminary Report. United States Geological Survey Bulletin 1107-F. 1962.

Palau Estevan, CV.; Arregui De La Cruz, F.; Carlos Alberola, MDM. (2012). Burst detection in water networks using principal component analysis. Journal of Water Resources Planning and Management. 138(1):47-54. doi:10.1061/(ASCE)WR.1943-5452.0000147.

Pratson, L., Hughes-Clarke, J., Anderson, M., Gerber, T., Twichell, D., Ferrari, R., Nittrouer, C., Beaudoin, J., Granet, J., and Crockett, J., 2008, Timing and patterns of basin infilling as documented in Lake Powell during a drought: Geology, v. 36, no. 11, p. 843–846.

Potter, L.D. and Drake, C.L. 1989. Lake Powell. Virgin flow to dynamo. University of New Mexico Press, Albuquerque, NM.

R Core Team (2013). R: A language and environment for statistical computing. R Foundation for Statistical Computing, Vienna, Austria.

Riba, I; DelValls, T.A.; Forja, J.M.; Gomez-Parra, A. (2002) Influence of the Azanaclollar mining spill on the vertical distribution of heavy metals in sediments from the Guadalquivir estuary (SW Spain). *Marin Pollution Bulletin* 44:39-47.

Rodriguez-Feriere, Lucia; Avasarala, Sumant; Abdul-Mehdi, S. Ali; Agnew, Diane; Hoover, Joseph H., Artyushkova, Kateryna; Latta, Drew E.; Peterson, Eric J.; Lewis, Johnnye; Crossey, Laura J.; Brearley, Adrian J.; Cerrato, Jose M. Post Gold King Mine Spill Investigation of Metal Stability in Water and Sediments of the Animas River Watershed. *Environmental Science and Technology,* 2016, 50(2), pp. 11539-11548.

Schemel, Laurence E.; Kimball, Briant A.; Bencala, Kenneth E. Colloid formation and metal transport through two mixing zones affected by acid mine drainage near Silverton Colorado. *Applied Geochemistry* 2000 12: 1003-1018

Stanford, J. A., & Ward, J. V. (1991, February). Limnology of Lake Powell and the chemistry of the Colorado River. In *Colorado River Ecology and Dam Management: Proceedings of a Symposium May 24-25, 1990 Santa Fe, New Mexico* (p. 75). National Academies Press.

Sullivan, Kate; Cyterski, Michael; Knightes, Chris; Kraemer, Stephen R.; Washington, John; Preto, Lourdes; Avant, Brian. 2017. Analysis of the Transport and Fate of Metals Released from the Gold King Mine in the Animas and San Juan Rivers. Environmental Protection Agency.

U.S. Bureau of Reclamation. December 2012. Colorado River Basin Water Supply and Demand Study. Reclamation: Managing Water in the West. United States Department of the Interior. [HYPERLINK "https://www.usbr.gov/watersmart//bsp/docs/finalreport/ColoradoRiver/CRBS_Executive_Summary_FINAL.pdf"]

U.S. Department of Energy, 2011. Natural contamination from the Mancos Shale. Prepared by the Environmental Sciences Laboratory Legacy Management, April 2011, LMS/S07480 ESL-RPT-2011-01.

U.S. Environmental Protection Agency. Bonita Peak Mining District Unincorporated, CO. Superfund Site. 2018. Retrieved from [HYPERLINK "https://cumulis.epa.gov/supercpad/SiteProfiles/index.cfm?fuseaction=second.Cleanup&id=0802497" \l "bkground"]

U.S. Environmental Protection Agency, 2017. Storage and Retrieval Database. Water Quality Data. National Water Quality Monitoring Council. Accessed from[HYPERLINK "https://www.waterqualitydata.us/portal/"]

U.S. Geological Survey (USGS), 2016. Determining water-quality trends using sediment cores, White Rock Lake, Dallas. United States Geological Survey. [HYPERLINK "https://pubs.usgs.gov/circ/circ1171/html/cores.htm"]

U.S. Geological Survey (USGS). Method 19 – 42 Element Inductively Coupled Plasma – Atomic Emissions Spectrometry – Mass Spectrometry (ICP-AES-MS), multi-acid (ICP-42). United States Geological Survey. Accessed 2018 from https://minerals.usgs.gov/science/analytical-chemistry/method19.html

U.S. Geological Survey (USGS). Water Data for the Nation. Nation Water Information System. Accessed 2018 from [HYPERLINK "https://waterdata.usgs.gov/nwis/rt"]

Valette-Silver, H.J., 1993. The use of sediment cores to reconstruct historical trends in contamination of estuarine and coastal sediments. Estuaries 16 (3B), 577–588.

606
607 Utah Division of Water Quality, Utah Department of Health, United States Geological Survey. 2018.
608 Integration of Long-term Impacts from Historical Mine Drainage and Episodic Release of Metals to
609 Sediments along the San Juan River and Lake Powell System in Utah. Available at: [HYPERLINK
610 "https://deq.utah.gov/legacy/topics/water-quality/gold-king-mine/index.htm" \t "_blank"]

611 Vernieu, William S. Effects of Reservoir Drawdown on Resuspension of Deltaic Sediments in Lake Powell.
612 Journal of Lake and Reservoir Management. 1997, 13(1): 67-78.

613
614 Wang, Yunqian; Yang, Liyuan; Kong, Linghao; Liu, Enfeng; Wang, Longfeng; Zhu, Jungru. (2015) Spatial
615 distribution, ecological risk assessment and source identification for heavy metals in surface sediments
616 from Dongping Lake, Shandong, East China. *Catena* 125(200-205).
617
618 Zielinski, Sarah. 2010. The Colorado River Runs Dry. *Smithsonian Magazine*. October 2010. Accessed at: [
619 HYPERLINK "https://www.smithsonianmag.com/science-nature/the-colorado-river-runs-dry-61427169/"
620]